Physica E 126 (2021) 114362

Contents lists available at ScienceDirect

Physica E: Low-dimensional Systems and Nanostructures

journal homepage: http://www.elsevier.com/locate/physe

Control of electronic and optical properties of a laser dressed double quantum dot molecule by lateral electric field

M.G. Barseghyan [a], V.N. Mughnetsyan [b], H.M. Baghramyan [c], F. Ungan [d], L.M. Pérez [e,*], D. Laroze [e]

[a] National University of Architecture and Construction of Armenia, Teryan 105, 0009, Yerevan, Armenia
[b] Department of Solid State Physics, Yerevan State University, Alex Manoogian 1, 0025, Yerevan, Armenia
[c] Istituto Italiano di Tecnologia, Via Eugenio Barsanti, 14, 73010, Arnesano, LE, Italy
[d] Faculty of Technology, Department of Optical Engineering, Sivas Cumhuriyet University, 58140, Sivas, Turkey
[e] Instituto de Alta Investigación, CEDENNA, Universidad de Tarapacá, Casilla 7D, Arica, Chile

A B S T R A C T

We study the confined states of a molecule formed by two laterally coupled quantum dots. The static electric field and incident plane wave laser field are considered with different polarization. The respective Shrödinger equation is obtained in the framework of the high-frequency limit of Floquet theory. It is shown that the electric field has a qualitative impact on the spatial symmetry of electronic states. An in-depth study of electric and laser field combined effects show a strong correlation between them. Additionally, we show that the linear, nonlinear and total optical absorption coefficients and relative refractive index of the considered structure can be effectively tuned by changing electric field strength and intense laser field parameter. Our results indicate the possibility of controlling the optical response of double quantum dots molecule for future applications in nanostructure-based quantum information science.

1. Introduction

An artificial molecule can be formed by two closely positioned quantum dots (QDs) resulting from the quantum tunneling. The coupling properties of such QD molecules (QDM) are in a focus of studies for optoelectronic and quantum information applications [1,2]. In particular, laterally coupled QDMs are candidates for constructing building blocks in the field of nanostructure-based quantum information science [3].

It is well known that the controllable tunnel coupling between QDs has technological importance [5]. Therefore, the tuning of coupling in double QDMs (DQDMs) has a great interest both from an experimental and theoretical point of view [4]. It has been demonstrated that by applying a lateral electric field on laterally coupled DQDM the electron localization can be readily controlled [3]. It was also pointed out that QDM can serve as single-photon emitters in a range of frequencies [6].

The effective controlling of one- and two-electron states in laterally coupled DQDMs with two-dimensional double parabolic confinement using the external electric and magnetic fields and changing the interdot distance have been investigated in Ref. [7]. In reverse, the application of a lateral electric field brings a superposition of localized states in separate QDs and a localized to a covalent diatomic molecular state transition.

Experiments show that the geometry of QDs in DQDMs is mostly elliptical rather than cylindrical [8]. We have already shown [9,10] that intense terahertz laser field (ILF) can induce and control the isotropic and anisotropic properties of quantum rings. Particularly, it can recover the physical properties in elliptical quantum rings that are specific to cylindrical symmetry. We have also shown that the electric field can cancel the degeneracy induced by IFL and, in turn, create new optical transitions [11]. Also, under ILF, Fock-Darwin states can be observed in anisotropic double QDs that are typical to single QDs with cylindrical symmetry [12]. In the current work, we analyze the effect of the electric field on the symmetry and coupling of laser field dressed electronic states in a DQDM. States are confined by parabolic confinement potential. A thorough analysis is done on the interplay between ILF and electric field effects. The key result is the possibility to control the symmetry of quantum states changing the direction and the strength of the electric field. ILF, in turn, can serve as means to supervise this change. The mentioned effects are also studied on the intraband optical properties of DQDM, such as on linear, nonlinear and total optical absorption coefficients and relative refractive index. The theoretical framework is given in Sec. 2, the analysis of results is presented in Sec. 3 and the conclusions are in Sec. 4.

* Corresponding author.
E-mail address: lperez@uta.cl (L.M. Pérez).

https://doi.org/10.1016/j.physe.2020.114362
Received 14 March 2020; Received in revised form 6 July 2020; Accepted 10 July 2020
Available online 15 August 2020
1386-9477/© 2020 Elsevier B.V. All rights reserved.

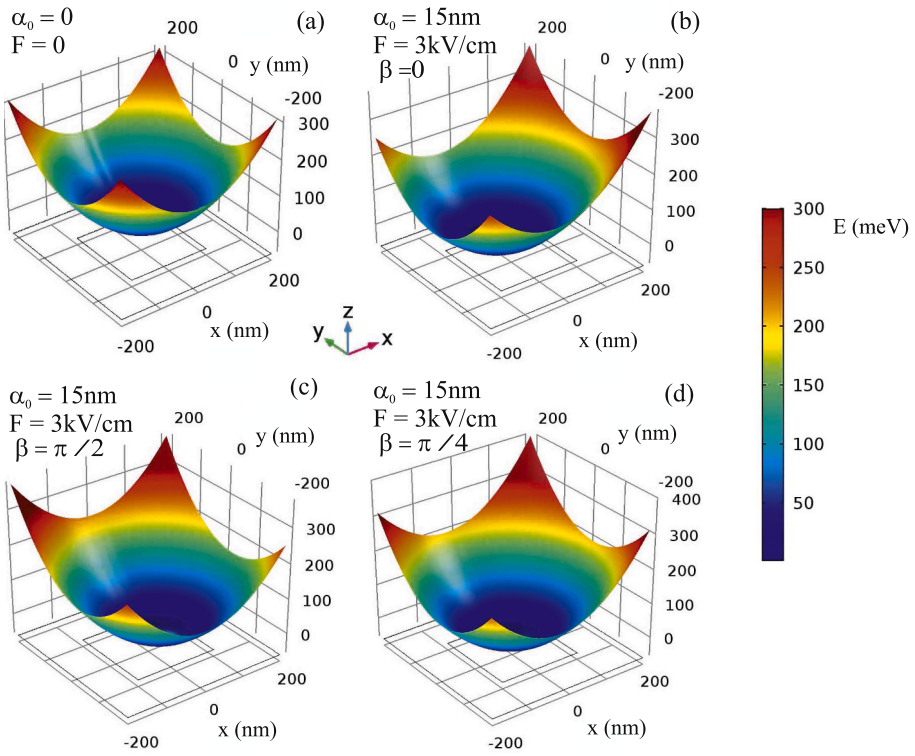


Fig. 1. Confining potential of DQDM as a function of the coordinates at $\hbar\omega_x = \hbar\omega_y = 3$ meV, $R = 10$ nm and $V_0 = 2$ meV for different values of laser and electric fields.

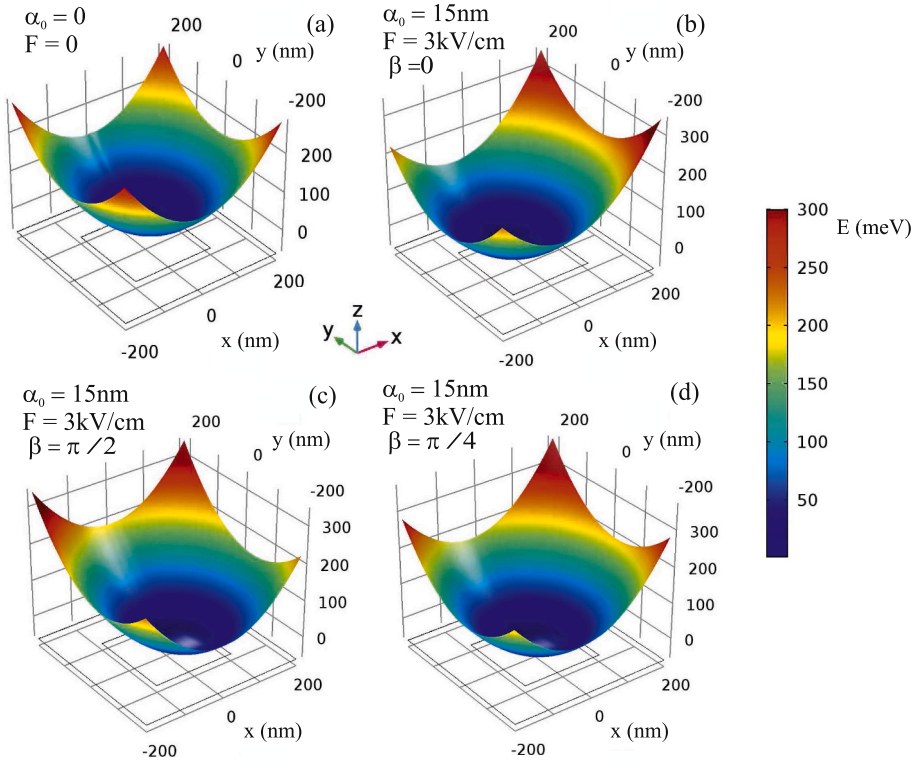


Fig. 2. Confining potential of DQDM as a function of the coordinates at $\hbar\omega_x = 3$ meV, $\hbar\omega_y = 2.7$ meV for different values of laser and electric fields.

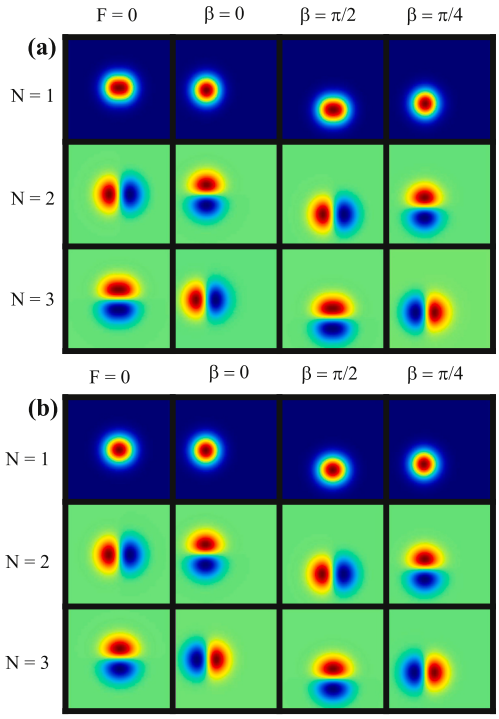


Fig. 3. Density plots of the probability density distributions for the first three electronic states. The first column of the table corresponds to the absence of an electric field, while other columns are for $F = 3$ kV/cm. The different directions of the electric field are mentioned by the corresponding value of β. Two different values of ILF parameter $\alpha_0 = 0$ (a) and $\alpha_0 = 15$ nm (b) are considered. The values of other parameters are fixed: $\hbar\omega_x = \hbar\omega_y = 3$ meV, $R = 10$ nm and $V_0 = 2$ meV.

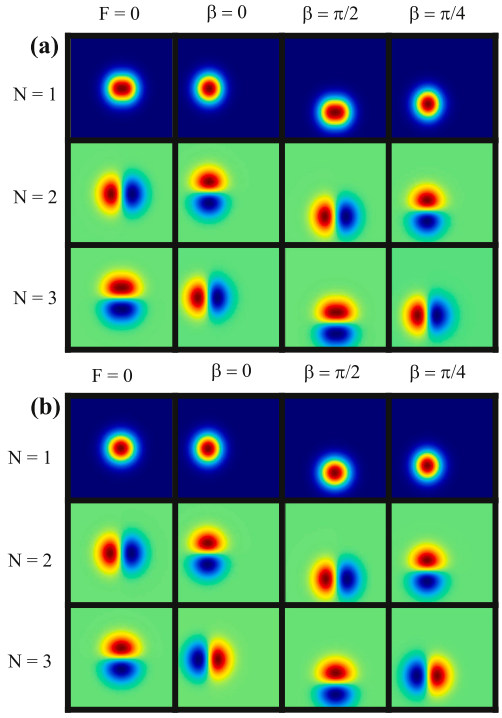


Fig. 4. Density plots of the probability density distributions for the first three electronic states. The first column of the table corresponds to the absence of an electric field, while other columns are for $F = 3$ kV/cm. The different directions of the electric field are mentioned by the corresponding value of β. Two different values of ILF parameter $\alpha_0 = 0$ (a) and $\alpha_0 = 15$ nm (b) are considered. The values of other parameters are fixed: $\hbar\omega_x = 3$ meV, $\hbar\omega_y = 2.7$ meV.

2. Theoretical model

The confinement potential of DQDM is a sum of two-dimensional parabolic potential and Gaussian barrier [13]:

$$V(x,y) = \frac{1}{2}m\left(\omega_x^2x^2 + \omega_y^2y^2\right) + V_0e^{-\frac{x^2}{R^2}}, \tag{1}$$

were $\omega_{x(y)}$ is the frequency of the confinement potential in $x(y)$ direction, R and V_0 are the width and height of the Gaussian barrier, respectively. The single electron Hamiltonian of the system can be written as:

$$\left[\frac{1}{2m}\left(\widehat{\mathbf{p}} - \frac{e}{c}\mathbf{A}(t)\right)^2 + V_F(x,y)\right]\Phi(x,y,t) = i\hbar\frac{\partial}{\partial t}\Phi(x,y,t), \tag{2}$$

where m is the electron effective mass, $\widehat{\mathbf{p}}$ is the momentum operator, e is the absolute value of the electron charge, $V_F(x, y) = V(x, y) - e\mathbf{F}\cdot\mathbf{r}$, where $\mathbf{F}$ is the electric field strength. The laser field is only time-dependent (dipole approximation is considered) and circularly polarized, therefore the vector potential of the ILF can be presented as:

$$\mathbf{A}(t) = A_0\left(\mathbf{e}_x\cos(\omega t) + \mathbf{e}_y\sin(\omega t)\right), \tag{3}$$

where $\mathbf{e}_x$ and $\mathbf{e}_y$ denote the unit vectors of the $x-$ and $y-$axes, respectively. Also, we select the electric field as $\mathbf{F} = F\left(\mathbf{e}_x\cos(\beta) + \mathbf{e}_y\sin(\beta)\right)$.

Since the laser field is only time-dependent [14], the Kramers-Henneberger transformation is performed [15] and Floquet theory in high-frequency limit is applied [16–21]. Taking into consideration the above mentioned physical reasoning, the following time-independent Schrödinger equation [11,22] is obtained:

$$\left[\frac{1}{2m}\widehat{\mathbf{p}}^2 + V_d - e\mathbf{F}\cdot\mathbf{r}\right]\Phi_d(x,y) = E_d\Phi_d(x,y). \tag{4}$$

In Eq. (4), $V_d = V_d(x, y, \alpha_0)$ is the time-averaged laser-dressed potential given by Ref. [14,23]:

$$V_d(x,y,\alpha_0) = \frac{\omega_0}{2\pi}\int_0^{\frac{2\pi}{\omega_0}} V(x+\alpha_0\cos(\omega_0 t), y+\alpha_0\sin(\omega_0 t))dt, \tag{5}$$

where $\alpha_0 = \left(8\pi e^2 I/m^2\varepsilon_h^{1/2}c\omega_0^4\right)^{1/2}$ is the amplitude of the quiver motion of the electron under the ILF, I and ω_0 stand for the intensity and the frequency of the ILF, respectively, and ε_h is the high-frequency dielectric constant.

On the other hand, it is well known that the density matrix approach allows deriving the linear and third-order nonlinear optical absorption coefficients, and relative refractive index change. The expressions for these quantities can be written as: [25,26]

$$\alpha^{(1)}(\omega) = \omega\sqrt{\frac{\mu}{\epsilon_r}}\,\frac{|M_{21}|^2\rho_s\Gamma}{(\Delta E - \hbar\omega)^2 + \Gamma^2}, \tag{6}$$

$$\alpha^{(3)}(\omega, I) = -2\omega\sqrt{\frac{\mu}{\epsilon_R}}\left(\frac{I}{\epsilon_0 n_r c}\right)\times \frac{|M_{21}|^4\rho_s\Gamma}{\left((\Delta E - \hbar\omega)^2 + \Gamma^2\right)^2}\left(1 - \frac{|\delta M|^2}{|2M_{21}|^2}\times \frac{(\Delta E - \hbar\omega)^2 - \Gamma^2 + 2\Delta E(\Delta E - \hbar\omega)}{(\Delta E)^2 + \Gamma^2}\right) \tag{7}$$

and

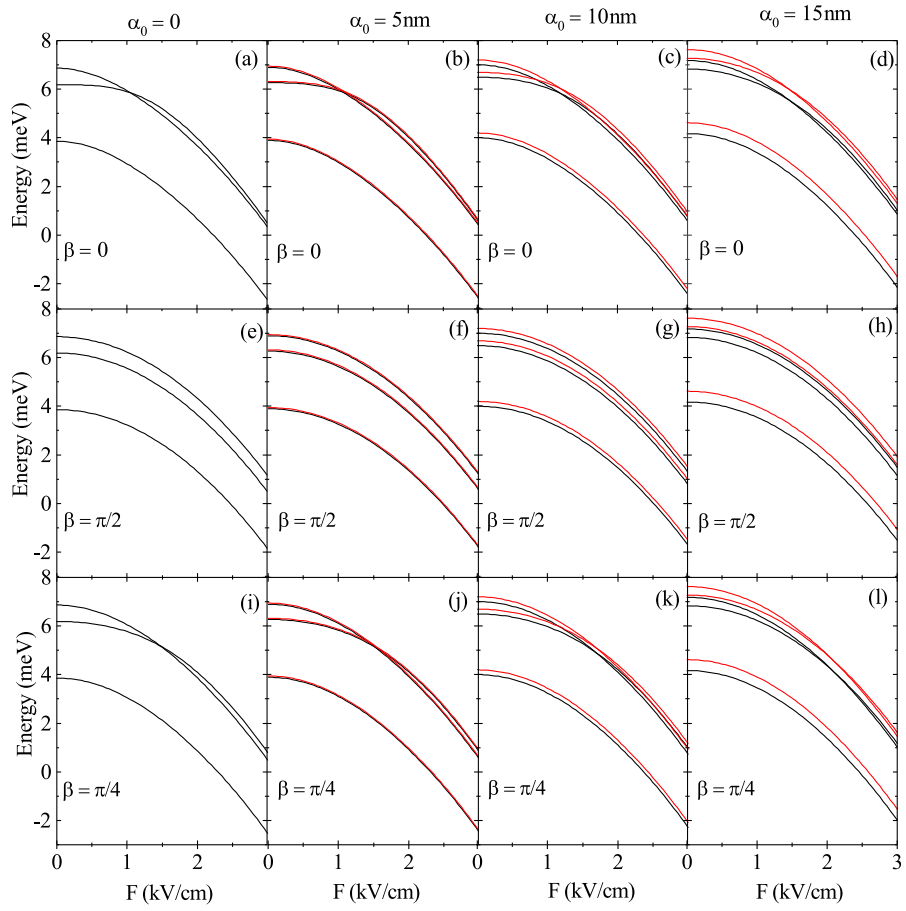


Fig. 5. Dependence of three lowest energy electron states on electric field with varying α_0 and electric field. Black and red lines represent the cases of linear and circular polarization of ILF, respectively. The rest of parameters are the same of Fig. 1. (For interpretation of the references to colour in this figure legend, the reader is referred to the Web version of this article.)

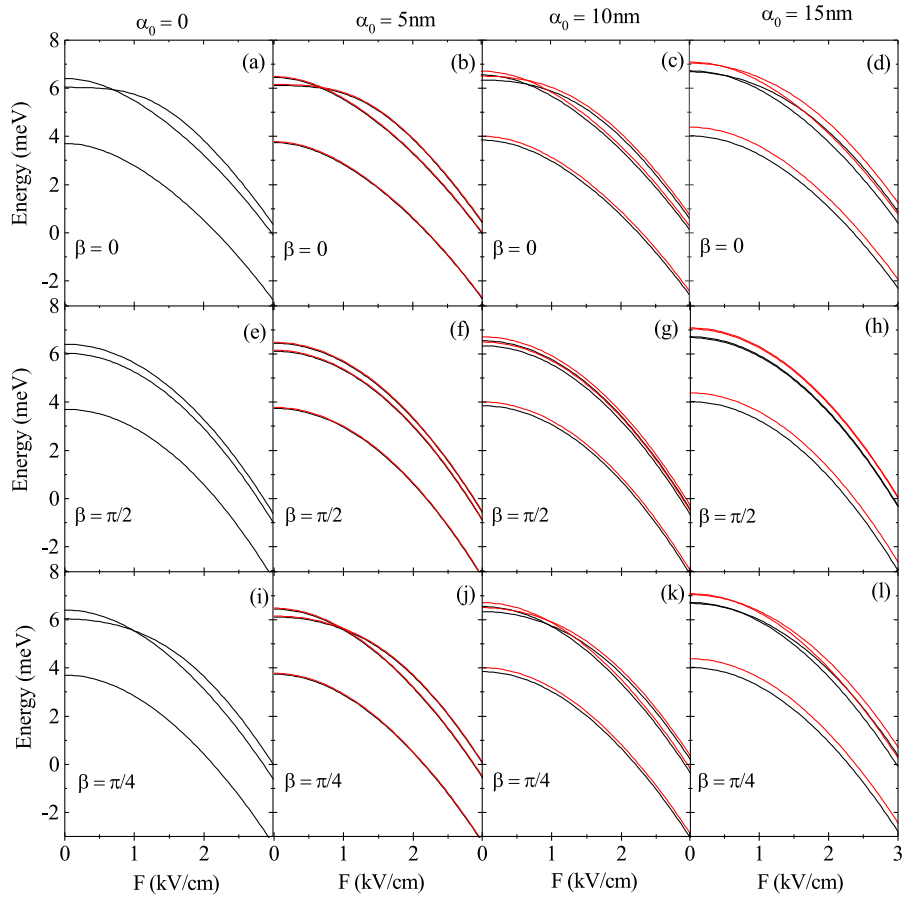


Fig. 6. Dependence of three lowest energy electron states on electric field with varying α_0 and electric field. Black and red lines represent the cases of linear and circular polarizations of ILF, respectively. Here the fixed parameters are: $R = 10$ nm, $V_0 = 2$ meV, $\hbar\omega_x = 3$ meV and $\hbar\omega_y = 2.7$ meV. (For interpretation of the references to colour in this figure legend, the reader is referred to the Web version of this article.)

$$\frac{\Delta n^{(1)}(\omega)}{n_r} = \frac{\rho_s |M_{10}|^2}{2n_r^2\epsilon_0} \frac{\Delta E - \hbar\omega}{(\Delta E - \hbar\omega)^2 + \Gamma^2}, \tag{8}$$

$$\frac{\Delta n^{(3)}(\omega, I)}{n_r} = -\frac{\mu c |M_{10}|^2}{4n_r^3\epsilon_0} \frac{\rho_s I}{((\Delta E - \hbar\omega)^2 + \Gamma^2)^2} \times \left[4(\Delta E - \hbar\omega)|M_{10}|^2 - \frac{(\delta M)^2}{(\Delta E)^2 + \Gamma^2}\{(\Delta E - \hbar\omega) \times (\Delta E(\Delta E - \hbar\omega) - \Gamma^2 - \Gamma^2(2(\Delta E) - \hbar\omega)\}\right], \tag{9}$$

where $M_{ab} = |\langle\psi_a|ex|\psi_b\rangle|$ is the matrix element of the dipole operator for x-polarization of the light, $\delta M = M_{22} - M_{11}$, and $\Delta E = E_2 - E_1$ is the energy difference between initial and final states. The total optical absorption coefficient, $\alpha(\omega, I)$, and relative refractive index change $\Delta n(\omega, I)/n_r$, can be written as the sum of linear and nonlinear components, respectively. Therefore, $\alpha(\omega, I) = \alpha^{(1)}(\omega) + \alpha^{(3)}(\omega, I)$ and $\Delta n(\omega, I)/n_r = (\Delta n^{(1)}(\omega) + \Delta n^{(3)}(\omega, I))/n_r$. In the expressions above, n_r is the refractive index of the structure, μ is the magnetic permeability, ϵ_0 is the dielectric permittivity of the vacuum, ω is the angular frequency of the incident photon, I is the intensity of electromagnetic field, Γ describes the broadening of the threshold energy, and ρ_s is the electron density in the structure.

3. Numerical results

We consider *GaAs* as the material for DQDM with $m = 0.067m_0$ (m_0 is the free electron mass), $\varepsilon_h = 10.5$, $V_0 = 2$ meV and $R = 10$ nm [13,24]. The eigenvalue equation Eq. (4) is solved in finite element method framework using COMSOL Multiphysics [27].

In Fig. 1 (symmetric - $\hbar\omega_x = \hbar\omega_y = 3$ meV) and Fig. 2 (asymmetric case - $\hbar\omega_x = 3$ meV, $\hbar\omega_y = 2.7$ meV) the confinement potential of the DQDM is given for varying ILF parameter α_0 and electric field strength F. As it is seen from the panels, in the case of laser-dressed DQDM, the barrier region for low laying electron states disappears. The electric field lowers the electron's potential, similar to the quantum-confined Stark effect in quantum wells [28].

In Fig. 3 the density plots of the first three quantum states are presented for undressed ((a) $\alpha_0 = 0$) and dressed ((b) $\alpha_0 = 15$ nm) for symmetric ($\hbar\omega_x = \hbar\omega_y = 3$ meV) DQDM. Considered values of electric field are $F = 0$ and $F = 3$ kV/cm. The non-zero electric field is directed along the x-axis ($\beta = 0$), y-axis ($\beta = \pi/2$) and the diagonal ($\beta = \pi/4$) directions. Comparing the ground states' density plots ($N = 1$) of undressed (Fig. 3 (a)) and dressed (Fig. 3 (b)) DQDM it is clear, that ILF always brings to the strengthening of electron localization at the center of the structure, which is caused by the lowering of the potential barrier between two dots. On the other hand, it is obvious that for all the considered values of parameters, the probability density distribution of an electron for each state moves in the opposite direction of the electric field. Additionally, one can note that by changing the electric field direction, the symmetry of the excited states ($N = 2$ and $N = 3$) can be totally changed. The exception is only the case when the direction of

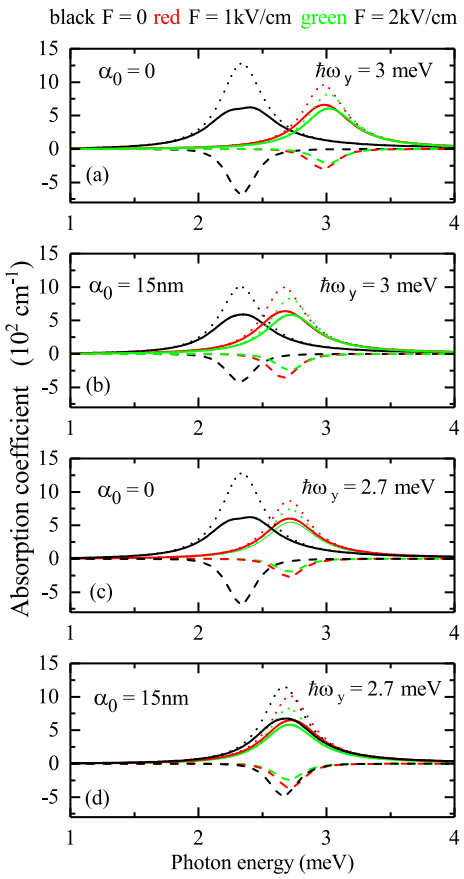


Fig. 7. Absorption coefficient as a function of photon energy: dotted lines are for $\alpha^{(1)}$, dashed lines are for $\alpha^{(3)}$ and solid lines are for α. Several values of electric field F, ILF parameter α_0 and confinement potential energy $\hbar\omega_y$ have been considered for $\hbar\omega_x = 3$ meV, $R = 10$ nm and $V_0 = 2$ meV.

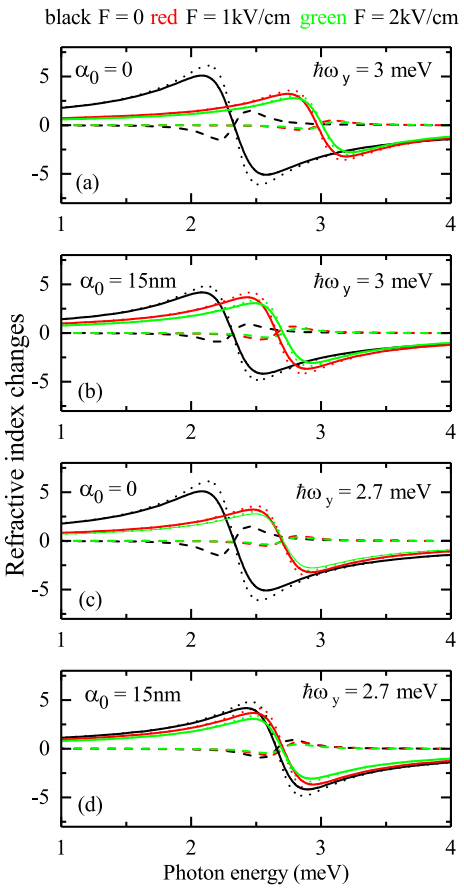


Fig. 8. Refractive index change as a function of photon energy: dotted lines are for $\Delta n^{(1)}/n_r$, dashed lines are for $\Delta n^{(3)}/n_r$ and solid lines are for $\Delta n/n_r$. Several values of electric field F, ILF parameter α_0 and confinement potential energy $\hbar\omega_y$ have been considered for $\hbar\omega_x = 3$ meV, $R = 10$ nm and $V_0 = 2$ meV.

electric field changes from y-axis to the direction along the diagonal ($\beta = \pi/4$) for $N = 3$ in the case of dressed DQDM. For the completeness of results density plots for the asymmetric case are also presented in Fig. 4.

The electric field dependence of the three lowest energy levels is given in Fig. 5. α_0 and electric field direction varying is considered with fixed $\hbar\omega_x = \hbar\omega_y = 3$ meV. The black and the red lines represent the case of linear and circular polarization of ILF, respectively. As in the previous figure, three different directions of the electric field ($\beta = 0$ (a)-(c), $\beta = \pi/2$ (e)-(h) and $\beta = \pi/4$ (i)-(l)) are considered. First of all, it is clear that with the increase of ILF parameter α_0, the energy levels corresponding to the circular polarization of ILF shift up with regard to ones for DQDM dressed by a linearly polarized ILF. The up-shift of energy levels is the result of the higher localization of the quantum states under the action of circularly polarized ILF. The crossings of the first and the second excited states for $\beta = 0$ and $\beta = \pi/4$ are caused by the symmetry changes in the wave functions of respective states (see Fig. 3). Moreover, as the electric field direction is changed from x-axis to diagonal one, as well as α_0 is incremented, the above-mentioned crossing points take place at higher electric field strength. If the electric field is y-axis oriented, the crossing between the first and the second excited states does not occur because of no change in the symmetry of wave functions.

Fig. 6 represents the same dependencies as in Fig. 5 but for anisotropic parabolic confinement: $\hbar\omega_x = 3$ meV, $\hbar\omega_y = 2.7$ meV. As in Fig. 5 the crossings of the first and the second excited states for $\beta = 0$ and $\beta = \pi/4$ are the result of the symmetry change of quantum states by electric field. However, in contrast to the case of isotropic confinement, one can observe a left-shift of the crossing points with the increase of the ILF parameter. This result is explained by the tendency of ILF to recover the isotropy of confinement potential.

Now, let us focus on the intraband optical properties. For this purpose, we fix the following parameters at $I = 10^3$ W/cm^2, $\Gamma = 0.4$ meV and $\rho_s = 3 \cdot 10^{16}$ cm^{-3}. In Figs. 7 and 8 the analysis of, respectively, linear and nonlinear absorption coefficient and relative refractive index is presented as a function of the incident photon energy for various values of α_0, $\hbar\omega_y$ ($\hbar\omega_x = 3$ meV in all curves) and F. The increment of F results in the blueshift of the spectrum and the decreasing of absorption and refractive index peak values in all cases. On the other hand, if electric field is off (black curves) only for $\hbar\omega_y = 2.7$ meV we observe a clear blueshift with the change of α_0. In addition, if $F \neq 0$, the increment of α_0 for $\hbar\omega_y = 3$ meV results in the redshift but we see almost no shift for $\hbar\omega_y = 2.7$ meV. Also, if we compare results for $\alpha_0 = 15$ nm, $F = 0$ condition results in the blueshift but if $F \neq 0$, then almost no shift is seen. The obtained results indicate that laser and static electric field can serve as potential means to control the linear and nonlinear optical properties of DQDM.

4. Final remarks

Summarizing, we have shown that the static electric field has a qualitative impact on the spatial symmetry of electronic states. Particularly, the change of the electric field direction can lead to the transformation of the quantum state symmetry, which can be controlled by an intense laser field. The symmetry transformation takes place also with the increment of the electric field of fixed direction. The later is expressed by the crossing of energy levels with electric field variation. Also, it is shown that the increase of laser field intensity leads to the right-shift of the crossing points of excited energy levels for isotropic

confinement, while a left-shift is observed for the quantum dot molecule with anisotropic confinement. The analysis of linear and nonlinear absorption and the relative refractive index has shown that the increased electric field influence results in the blueshift of the peaks, while by affecting the symmetry of the structure (by $\hbar\omega_y$) and varying α_0 both blue and redshift of peaks have been obtained. We hope the obtained results help to better understand the electronic and optical properties of double quantum dot molecule and similar nanostructures under the influence of intense laser and static electric fields.

Credit author statement

All the authors have equally contributed.

Declaration of competing interest

The authors declare that they have no known competing financial interests or personal relationships that could have appeared to influence the work reported in this paper.

Acknowledgments

MGB and VNM acknowledge the financial support by the Armenian State Committee of Science (Project no. 18T-1C223). LMP and DL acknowledge partial financial support from FONDECYT 1180905. DL acknowledges partial financial support from Centers of excellence with BASAL/CONICYT financing, Grant AFB180001, CEDENNA.

References

[1] M.F. Doty, J.I. Climente, M. Korkusinski, M. Scheibner, A.S. Bracker, P. Hawrylak, D. Gammon, Phys. Rev. Lett. 102 (2009), 047401.
[2] A.N. Vamivakas, C.-Y. Lu, C. Matthiesen, Y. Zhao, S. Fält, A. Badolato, M. Atatüre, Nature 467 (2010) 297.
[3] G.J. Beirne, C. Hermannstädter, L. Wang, A. Rastelli, O.G. Schmidt, P. Michler, Phys. Rev. Lett. 96 (2006) 137401.
[4] R.M. Abolfath, P. Hawrylak, Phys. Rev. Lett. 97 (2006) 186802.
[5] X. Zhou, M. Doty, J. Appl. Phys. 116 (2014) 163101.
[6] A.J. Shields, Nat. Photon. 1 (2007) 215.
[7] V. Popsueva, R. Nepstad, T. Birkeland, M. Førre, J.P. Hansen, E. Lindroth, E. Waltersson, Phys. Rev. B 76 (2007), 035303.
[8] J. Wu, Z.M. Wang, Quantum Dot Molecules, Springer-Verlag, New York, 2014.
[9] T. Chakraborty, A. Manaselyan, M. Barseghyan, D. Laroze, Phys. Rev. B 97 (2018), 041304(R).
[10] H.M. Baghramyan, M.G. Barseghyan, A.A. Kirakosyan, J.H. Ojeda, J. Bragard, D. Laroze, Sci. Rep. 8 (2018) 6145.
[11] H.M. Baghramyan, M.G. Barseghyan, D. Laroze, Sci. Rep. 7 (2017) 10485.
[12] M.G. Barseghyan, H.M. Baghramyan, A.A. Kirakosyan, D. Laroze, Physica E 116 (2020) 113758.
[13] W. Dybalski, P. Hawrylak, Phys. Rev. B 72 (2005) 205432.
[14] M. Gavrila, Atoms in Intense Laser Fields, Academic, New York, 1992.
[15] W.C. Henneberger, Phys. Rev. Lett. 21 (1968) 838.
[16] M. Gavrila, J.Z. Kaminski, Phys. Rev. Lett. 52 (1984) 613.
[17] M. Pont, N.R. Walet, M. Gavrila, C.W. McCurdy, Phys. Rev. Lett. 61 (1988) 939.
[18] E.C. Valadares, Phys. Rev. B 41 (1990), 1282(R).
[19] M. Gavrila, J. Phys. B Atom. Mol. Opt. Phys. 35 (2002) R147.
[20] S. Ganichev, W. Prettl, Intense Terahertz Excitation of Semiconductors, Oxford University Press, 2006.
[21] M. Bukov, L. D'Alessio, A. Polkovnikov, Adv. Phys. 64 (2015) 139.
[22] M.G. Barseghyan, A. Manaselyan, A.A. Kirakosyan, L.M. Pérez, D. Laroze, Physica E 117 (2020) 113807.
[23] J.A. Vinasco, A. Radu, E. Niculescu, M.E. Mora-Ramos, E. Feddi, V. Tulupenko, R. L. Restrepo, E. Kasapoglu, A.L. Morales, C.A. Duque, Sci. Rep. 9 (2019) 1427.
[24] S. Adachi (Ed.), Handbook on Physical Properties of Semiconductors. Volume 2: Compound Semiconductors, Springer, Boston, MA, 2004.
[25] R.L. Restrepo, M.G. Barseghyan, M.E. Mora-Ramos, C.A. Duque, Physica E 51 (2013) 48.
[26] F. Ungan, M.E. Mora-Ramos, M.G. Barseghyan, L.M. Pérez, D. Laroze, Physica E 114 (2019) 113647.
[27] COMSOL Multiphysics, V. 5.3b, COMSOL AB, Stockholm, Sweden.
[28] D.A.B. Miller, D.S. Chemla, T.C. Damen, Phys. Rev. Lett. 53 (1984) 2173.